ELSEVIER

Biochemical Pharmacology 64 (2002) 527–541

Biochemical Pharmacology

Analysis of oxidative processes and of myelin figures formation before and after the loss of mitochondrial transmembrane potential during 7β-hydroxycholesterol and 7-ketocholesterol-induced apoptosis: comparison with various pro-apoptotic chemicals

Carole Miguet-Alfonsi[a], Céline Prunet[a], Serge Monier[a], Ginette Bessède[a], Stéphanie Lemaire-Ewing[a], Arnaud Berthier[a], Franck Ménétrier[b], Dominique Néel[a], Philippe Gambert[a], Gérard Lizard[a,*]

[a]*CHU/Hôpital du Bocage, Laboratoire de Biochimie Médicale, Inserm U498, BP 1542, 21034 Dijon Cedex, France*
[b]*IFR 100 Inserm, Centre de Microscopie Préparative Appliqué à la Biologie et à la Médecine, Faculté de Médecine, 7 Bd Jeanne d'Arc, 21033 Dijon Cedex, France*

Received 26 November 2001; accepted 23 April 2002

Abstract

Among oxysterols oxidized at C7 (7α-, 7β-hydroxycholesterol, and 7-ketocholesterol) 7β-hydroxycholesterol and 7-ketocholesterol are potent inducers of cell death and probably play central roles in atherosclerosis. As suggested by our previous investigations, 7-ketocholesterol might be a causative agent of vascular damage by inducing apoptosis and enhancing superoxide anion ($O_2^{\bullet -}$) production. To determine the precise relationships between cytotoxicity and oxidative stress, the ability of oxysterols oxidized at C7 to induce apoptosis, to stimulate $O_2^{\bullet -}$ production and to promote lipid peroxidation was compared with different pro-apoptotic chemicals: antitumoral drugs (VB, Ara-C, CHX, and VP-16) and STS. All compounds, except 7α-hydroxycholesterol, induced apoptosis characterized by the occurrence of cells with fragmented and/or condensed nuclei, loss of mitochondrial potential, caspase-3 activation, PARP degradation, and internucleosomal DNA fragmentation. The highest proportion of apoptotic cells was found with antitumoral drugs and STS, whereas the highest overproduction of $O_2^{\bullet -}$ detected before and after the loss of mitochondrial potential was obtained with 7β-hydroxycholesterol and 7-ketocholesterol. Overproduction of $O_2^{\bullet -}$ was always correlated with enhanced lipid peroxidation. Vit E was only capable to significantly counteract apoptosis and oxidative stress induced by 7β-hydroxycholesterol, 7-ketocholesterol, VB and STS. By electron and fluorescence microscopy, myelin figures evocating autophagic vacuoles were barely observed under treatment with 7β-hydroxycholesterol and 7-ketocholesterol, and their formation occurring before the loss of mitochondrial potential was reduced by Vit E. In the presence of 7α-hydroxycholesterol, no enhancement of $O_2^{\bullet -}$ production, no lipid peroxidation, and no formation of myelin figures were observed. Collectively, our data demonstrate, that there can be a more or less important stimulation of oxidative stress during apoptosis. They also suggest that enhancement of $O_2^{\bullet -}$ production associated with lipid peroxidation during 7β-hydroxycholesterol and 7-ketocholesterol-induced apoptosis could contribute to *in vivo* vascular injury, and that myelin figures could constitute suitable markers of oxysterol-induced cell death.

Keywords: Apoptosis; Myelin figures; Oxysterol; Lipid peroxidation; Superoxide anions; Autophagic vacuoles

1. Introduction

Oxysterols are oxygenated cholesterol derivatives which constitute a family of natural compounds present in plants and animals [1,2]. These compounds bear in addition to the C3β-hydroxyl of cholesterol, one or several oxygenated moieties on the sterol nucleus or on the side chain [3], and they result either from auto-oxidation of cholesterol in air

* Corresponding author. Tel.: +33-3-80-29-38-53; fax: +33-3-80-29-36-61.
E-mail address: gerard.lizard@u-bourogne.fr (G. Lizard).

Abbreviations: Ara-C, cytosine β-D-arabinofuranoside; CHX, cycloheximide; GSH, glutathione; HE, hydroethidine; MDA, malondialdehyde; MDC, monodansylcadaverine; NAC, *N*-acetylcysteine; Oxidized LDL, oxLDL; PARP, poly(ADP-ribose)polymerase; PBS, phosphate buffered saline; ROS, reactive oxygen species; STS, staurosporine; TBA, thiobarbituric acid; VB, vinblastine; VP-16, etoposide.

0006-2952/02/$ – see front matter © 2002 Elsevier Science Inc. All rights reserved.
PII: S0006-2952(02)01110-3

[4], enzyme-catalyzed transformation of cholesterol in various cell species [5], or oxidation of cholesterol by free radicals generated by xenobiotics or by ionizing radiation [6]. To date, there is evidence that oxysterols are absorbed and incorporated into chylomycrons [7]. As oxysterols have been detected at increased concentrations in plasma [8] and in atherosclerotic plaques [9–11] from hypercholesterolemic patients, it is now well admitted that these compounds probably play important roles in atherosclerosis [12]. At least 60 oxysterols have been identified [13] and some of them, mainly 7β-hydroxycholesterol and 7-ketocholesterol, are cytotoxic at micromolar concentrations towards a wide number of normal and tumoral cells in culture by inducing an apoptotic process of cell death [14–16] characterized by the occurrence of cells with fragmented and/or condensed nuclei, and by various cellular dysfunctions: phosphatidylserine externalization, loss of mitochondrial transmembrane potential, cytosolic release of cytochrome *c*, activation of caspase-9 and -3 with subsequent degradation of poly(ADP-ribose)polymerase (PARP), and increased accumulation of cellular C16:0 and C24:1 ceramide species [17,18]. Noteworthy, 7α-hydroxycholesterol was not cytotoxic, underlying the complexity of the biological activities of oxysterols oxidized at C7 (7α-, 7β-hydroxycholesterol, and 7-ketocholesterol) [17]. In addition, 7-ketocholesterol-induced apoptosis is associated with an enhanced production of reactive oxygen species (ROS) detected by flow cytometry with the dyes 2′-7′-dichlorofluorescin-diacetate [19] and hydroethidine (HE) [20]. Since 7-ketocholesterol has the ability to stimulate ROS production, we asked whether this phenomenon occurred with the two other oxysterols oxidized at C7 (7α- and 7β-hydroxycholesterol) which are also found at increased concentrations in atherosclerotic lesions [3,9]. In addition, in order to elucidate the relationships between apoptosis and oxidative stress, analysis of ROS hyperproduction in 7α-, 7β-hydroxycholesterol, and 7-ketocholesterol-treated cells was performed in comparison with various pro-apoptotic chemicals from unrelated structures and mechanisms.

To this end, human U937 promonocytic leukemia cells [21] were treated with either 7α-, 7β-hydroxycholesterol, or 7-ketocholesterol, with the antibiotic staurosporine (STS), which is a non-isoform specific protein kinase C inhibitor [22], or with the following antitumoral drugs: vinblastine (VB), which is an alkaloid blocking the formation of microtubules involved in the elaboration of the mitotic spindle [23], cytosine β-D-arabinofuranoside (Ara-C), which is an antimetabolite structurally similar to pyrimidic bases and which incorporates into DNA leading to inhibition of DNA synthesis [24], cycloheximide (CHX), which is a protein synthesis inhibitor [25], and etoposide (VP-16), which belongs to the class of epipodophyllotoxins and which is an inhibitor of topoisomerase II [26]. After treatment with these different compounds, apoptotically dying cells were quantified by determining the proportion of cells with fragmented and/or condensed nuclei after nuclei staining with Hoechst 33342 [15]. Apoptosis was also characterized by immunocytochemistry and Western blot with antibodies recognizing activated caspase-3 and cleaved PARP [27,28]. Simultaneously, ROS hyperproduction was determined by flow cytometry with the use of HE which permits the identification of superoxide anion ($O_2^{\bullet -}$ on whole cells [29] as well as by a fluorimetric reaction with thiobarbituric acid (TBA) which mainly allows the quantification of malondialdehyde (MDA), an endproduct of lipid peroxidation [30]. As myelin figures, evocating autophagic vacuoles by their multilamellar structure [31] were previously observed by transmission electron microscopy on human vascular endothelial cells treated with 7-ketocholesterol [32], the autofluorescent compound monodansylcadaverine (MDC) which is considered as a specific marker of autophagic vacuoles [33,34] was used to precise the origin of these structures by fluorescence microscopy. Moreover, by using transmission electron microscopy and fluorescence microscopy; we attempted to determine whether these abnormal cellular structures were specific to 7-ketocholesterol-treated cells or whether they could be detected with other pro-apoptotic molecules, especially those inducing an oxidative stress.

As Vitamin E (Vit E) has been described to reduce lipid peroxide-scavenging activity of plasma [35] as well as to protect against atherosclerosis [36], and as we previously reported that Vit E was capable to counteract 7-ketocholesterol-induced apoptosis [20], the ability of this antioxidant to block the generation of $O_2^{\bullet -}$, to decrease lipid peroxidation, to reduce the formation of myelin figures, and to inhibit apoptosis was also investigated when U937 cells were treated either with oxysterols (7β-hydroxycholesterol, 7-ketocholesterol), antitumoral drugs from unrelated structures and mechanisms (VB, Ara-C, CHX, VP-16), or STS.

Under these conditions, an enhanced production of $O_2^{\bullet -}$ as well as myelin figures, corresponding probably to autophagic vacuoles, were observed during 7β-hydroxycholesterol and 7-ketocholesterol-induced apoptosis, but not with 7α-hydroxycholesterol, which had no cytotoxic effect, and an important lipid peroxidation process was also found when the cells were cultured with these oxysterols. With the different pro-apoptotic chemicals studied (VB, Ara-C, CHX, VP-16, and STS), important variations in the overproduction of $O_2^{\bullet -}$ and lipid peroxidation were revealed, but myelin figures were never detected no matter which chemicals were investigated.

2. Materials and methods

2.1. Chemicals and reagents

The 7α- and 7β-hydroxycholesterol were purchased from Steraloids, whereas 7-ketocholesterol was purchased

from Sigma; the purities of these oxysterols were determined to be 100% by gaseous phase chromatography-mass spectrometry. Antitumoral drugs (VB, Ara-C, CHX, and VP-16), and STS were obtained from Sigma. Hoechst 33342 and MDC were purchased from Sigma, and HE was obtained from Molecular Probes. TBA was obtained from Sigma. 3,3′-Diaminobenzidine was obtained from Dako. The mounting media Fluoprep and Fukitt were purchased from Biomérieux and CML, respectively. Culture media, supplements and fetal calf serum were purchased from Gibco BRL.

2.2. Cells and cell culture

U937 cells were grown in suspension in culture medium consisting of RPMI 1640 medium, 2 mM L-glutamine (Gibco), and antibiotics (100 U/mL penicillin, 100 μg/mL streptomycin) (Gibco) supplemented with 10% (v/v) heat-inactivated fetal calf serum. Cells were seeded at 5×10^5/mL of culture medium, passaged twice a week and incubated at 37° under a 5% CO_2/95% air atmosphere.

2.3. Cell treatments

In all experiments, initial solutions of 7α-, 7β-hydroxycholesterol and 7-ketocholesterol were prepared at a concentration of 800 μg/mL as previously described [17]. The initial oxysterol solutions were made by dissolving 800 μg of oxysterol in 50 μL of absolute ethanol, 950 μL of culture medium were further added, and the solution was sonicated. The 7α-, 7β-hydroxycholesterol and 7-ketocholesterol were introduced in the culture medium at the beginning of the culture at final concentrations of 80 μg/mL (200 μM), 20 μg/mL (50 μM), and 40 μg/mL (100 μM), respectively. Stock solutions of VB (10 μM), Ara-C (50 mM), and VP-16 (20 mM) were prepared by dilution in dimethylsulfoxide (Sigma). Stock solutions of CHX (35 mM) and STS (100 μM) were obtained by dilution in culture medium. Further dilutions were performed in culture medium in order to obtain the following final concentrations: VB (11 nM), Ara-C (50 μM), CHX (178 μM), VP-16 (50 μM), and STS (0.5 μM). The incubation times with the various compounds investigated were the followings: 7α-hydroxycholesterol (10, 24 hr), 7β-hydroxycholesterol (10, 18 hr), 7-ketocholesterol (10, 24 hr), VB (2, 24 hr), Ara-C (2, 24 hr), CHX (2, 18 hr), VP-16 (1, 5 hr), and STS (2, 18 hr). A stock solution of Vit E (Sigma) corresponding to DL-α-tocopherol (purity 95%) was prepared at 100 mM in ethanol, and diluted in the culture medium to obtain a 100 μM final concentration. In all experiments, Vit E was introduced in the culture medium at the beginning of the culture, and oxysterols (7β-hydroxycholesterol, 7-ketocholesterol), antitumoral drugs (VB, Ara-C, CHX, VP-16), or STS were added 1 hr later.

2.4. Identification and quantification of apoptotic cells after nuclei staining with Hoechst 33342

Nuclear morphology was analyzed by fluorescence microscopy after staining with Hoechst 33342. Apoptotic cells were characterized by nuclear condensation of chromatin and/or nuclear fragmentation [15]. Hoechst 33342 was prepared in distilled water at 1 mg/mL and added to the culture medium at a final concentration of 10 μg/mL. After 30 min of incubation at 37°, cells were collected by centrifugation, and resuspended at a concentration of 10^6 cells/mL in cold PBS containing 2% (w/v) paraformaldehyde. Cell deposits of 40,000 cells were applied to glass slides by cytocentrifugation (5 min, 300 *g*) with a cytospin 2 (Shandon), mounted in Fluoprep, coverslipped and stored in the dark at 4°. The morphology of cell nuclei was observed with an Axioskop right microscope (Zeiss) by using UV light excitation, and 300 cells were examined for each sample.

2.5. Identification of autophagic vacuoles after staining with monodansylcadaverine

The presence of autophagic vacuoles was analyzed by fluorescence microscopy after staining with monodansylcadaverin (MDC) [33,34]. MDC (λE_x max 340 nm, λE_m max 530 nm) was prepared at 0.1 M in DMSO and added to the culture medium at a final concentration of 0.1 mM. After 30 min of incubation at 37°, cells were collected by centrifugation, resuspended in culture medium (2×10^6 cells/mL), and 50 μL of cell suspension were applied to glass slides, coverslipped and immediately examined under an Axioskop right microscope (Zeiss) by using UV light excitation. For each sample, 300 cells were examined.

2.6. Identification of the active form of caspase-3 and of poly(ADP-ribose)polymerase degradation by immunocytochemistry and by Western blot analysis

By immunohistochemistry, detection of active caspase-3 and of cleaved PARP was performed on cell deposits of 40,000 cells applied to silanated glass slides by cytocentrifugation for 5 min at 300 *g* with a cytospin 2 (Shandon) and stored at 20°. For immunohistochemistry, after blocking the endogenous peroxidase activity with 0.33% H_2O_2 for 15 min at room temperature, the slides were washed in phosphate buffered saline (PBS) adjusted to pH 7.2 (PBS) and incubated for 15 min at room temperature with normal goat serum diluted 1:30 in PBS. After three washes in PBS, the slides were thereafter incubated either for 1 hr at room temperature with the polyclonal rabbit anti-active caspase-3 antibody (Pharmingen) diluted 1 μg/mL in PBS or overnight at 4° with the polyclonal rabbit antibody raised against cleaved PARP (New England Biolabs) diluted 1:100 in PBS. After three washes in PBS, the slides were

successively incubated for 15 min at room temperature with a biotinylated goat anti-rabbit IgG (BIOSPA) diluted 1:250 in PBS, washed three times in PBS, and incubated for 15 min with streptavidin peroxidase complex (BIOSPA) diluted 1:250 in PBS. After washing in PBS, peroxidase activity was revealed with 3,3′-diaminobenzidine for 5–10 min at room temperature. Counterstaining was performed with hemalun-eosin, and the slides were mounted in Eukitt, and stored at room temperature until examination with an Axioskop right microscope (Zeiss). The controls used included the omission of the primary antibodies (conjugated controls); under this condition, no non-specific signals were observed. Cells were examined under an Axioskop microscope (Zeiss) and images were digitalized with an image analysis system (Biocom).

By Western blot, degradation of caspase-3, and cleavage of PARP were analyzed as previously described on Ripa buffer (150 mM NaCl, 50 mM Tris–HCl pH 8.0, 0.1% SDS, 0.5% Na desoxycholate) extracts and on total cellular extracts, respectively [17]. The protein concentrations were measured by using bicinchoninic acid reagent (Pierce) according to the method of Smith *et al.* [37]. Thirty to 50 μg of protein were incubated in loading buffer (125 mM Tris–HCl, pH 6.8, 10% β-mercapto-ethanol, 4.6% SDS, 20% glycerol, 5 M urea and 0.003% bromophenol blue), boiled for 3 min, separated by SDS-polyacrylamide gel electrophoresis and electroblotted onto polyvinylidine difluoride membrane (Biorad). After blocking non-specific binding sites overnight by 5% non-fat milk in TPBS (PBS, Tween 20 0.1%), the membranes were incubated for 2 hr at room temperature with various primary antibodies: a rabbit polyclonal antibody recognizing both whole caspase-3 (32 kDa) as well as large (17 kDa) and small (12 kDa) subunits diluted at 1/5000 (BIOMOL Research Laboratories), and a rabbit polyclonal antibody directed against the uncleaved (115 kDa) and the cleaved (85 kDa) forms of PARP used at 1/1000 (Upstate Biotechnology). All antibodies were diluted in TPBS. After two washes in TPBS, the membranes were incubated with horseradish peroxidase-conjugated swine anti-rabbit (Dako) diluted 1/3000 for 1 hr at room temperature and washed twice in TPBS. Autoradiography of the immunoblots was performed using an enhanced chemoluminescence detection kit (Amersham). Autoradiographies were digitized using an image analysis system (Biocom). Each experiment was repeated three times with identical results.

2.7. Fluorogenic assay for caspase-3 protease activity

To assess caspase-3 activity, the cleavage of Ac-DEVD-AMC-7-amino-4-methylcoumarin (Ac-DEVD-AMC) was measured according to the manufacturer procedure with the Quanti Pak™ kit (BIOMOL Research Laboratories) in U937 cells incubated for various periods of times in their culture medium in the absence or presence of 7α-hydroxycholesterol (200 μM, 24 hr), 7β-hydroxycholesterol (50 μM, 18 hr), 7-ketocholesterol (100 μM, 24 hr), VB (11 nM, 24 hr), Ara-C (50 μM, 24 hr), CHX (178 μM, 18 hr), VP-16 (50 μM, 5 hr) or STS (0.5 μM, 18 hr). Briefly, at the end of the incubation time, cells were counted, harvested by centrifugation (1000 *g*, 4°, 10 min), and resuspended to 5×10^7 cells/mL of ice-cold lysis buffer (50 mM-(*N*-[(2-hydroxyethyl] piperazine-*N*′-[2-ethanesulfonic acid]) (HEPES), pH 7.4, 0.1% (3[(3-chloramidopropyl) dimethylammonio]-1-propane-sulfonate) (CHAP S), 1 mM dithiothreitol (DTT), 0.1 mM ethylenediaminetetraacetic acid (EDTA), 1% Triton X-100). After 10 min of incubation in an ice bath, cells were centrifuged (10,000 *g*, 4°, 10 min), and the supernatant (cytosolic extract) was collected. For each assay, the cytosolic extract (10 μL) was mixed with 80 μL of assay buffer (50 mM HEPES, pH 7.4, 100 mM NaCl, 0.1% CHAPS, 10 mM DTT, 1 mM EDTA, 10% glycerol), and with 10 μL of substrate solution (2 mM Ac-DEVD-AMC). The fluorescence of the liberated AMC was measured at room temperature at 2 min intervals for 40 min using a Victor^2 microspectrofluorometer (Wallac) (λE_x 484 nm, λE_m 501 nm) in order to determine the specific activity of the assay. In these conditions, three independent experiments were performed in triplicate.

2.8. Transmission electron microscopy

For transmission electron microscopy 20×10^6 cells were fixed for 1 hr with 2% glutaraldehyde prepared in a 0.1 M cacodylate buffer (pH 7.4), postfixed in osmium tetroxide, dehydrated with graded ethanol series, and finally embedded in Epon. Sections were stained with uranyl acetate and lead citrate, and were examined with an H600 electron microscope (Hitachi).

2.9. DNA fragmentation assay on agarose gel

Cellular DNA extraction and DNA fragmentation assay were carried out as previously reported [19,38]. After electrophoresis on 1.8% agarose, gels were examined under ultraviolet light and photographed or digitalized with an analyzing system (Biocom).

2.10. Flow cytometric measurement of the mitochondrial transmembrane potential ($\Delta\Psi_m$) with the cationic lipophilic dye $DiOC_6(3)$

The mitochondrial transmembrane potential ($\Delta\Psi_m$) was measured with 3,3′-dihexyloxacarbocyanine iodide ($DiOC_6(3)$: λE_x max 484 nm, λE_m max 501 nm) (Molecular Probes) used at 40 nM final concentration. This cyanine dye, which accumulates in the mitochondrial matrix under the influence of the $\Delta\Psi_m$ [39], was initially prepared at 1 mM in DMSO (Sigma), and further diluted in distilled water in order to obtain a 20 μM intermediate solution. To obtain a 40 nM final concentration, 2 μL of

this intermediate solution were added to cell suspensions adjusted to 2×10^6 cells/mL, and after 15 min of incubation at 37°, $DiOC_6(3)$ mitochondrial transmembrane potential related fluorescence was immediately recorded by flow cytometry with a GALAXY flow cytometer (Partec). The green fluorescence was collected through a 520/10 nm band pass filter, and the fluorescent signals were measured on a logarithmic scale of four decades of log. For each sample, 10,000 cells were acquired and the data were analyzed with Flow Mate software (Partec).

2.11. Flow cytometric measurement of the production of $O_2^{\bullet -}$ with hydroethidine

The production of superoxide anion ($O_2^{\bullet -}$) was detected with HE on U937 cells cultured in the absence, or in the presence of oxysterols oxidized at C7 (7α-hydroxycholesterol (200 μM), 7β-hydroxycholesterol (50 μM), and 7-ketocholesterol (100 μM)), antitumoral drugs (VB (11 nM), Ara-C (50 μM), CHX (178 μM), and VP-16 (50 μM)), or STS (0.5 μM). HE is a non-fluorescent compound which can diffuse through cell membranes, and which is rapidly oxidized in ethidium under the action of $O_2^{\bullet -}$ [29]. HE (excitation: 488 nm; emission: 525 nm) was initially prepared at 10 mM in DMSO [40] and used at 2 μM final concentration on cell samples of 1×10^6 cells/mL of RPMI 1640 medium containing 10% fetal calf serum. After 15 min of incubation at 37°, cells were kept on ice until analysis by flow cytometry with a GALAXY flow cytometer (Partec). The green fluorescence was collected through a 520/10 nm band pass filter, and the fluorescent signals were measured on a logarithmic scale of four decades of log. For each sample, 5000 cells were acquired and the data were analyzed with Flow Mate software (Partec).

2.12. Fluorometric quantification of lipid peroxidation by thiobarbituric acid reaction

MDA, which is an endproduct of lipid peroxidation, was detected by a fluorimetric assay with the use of TBA. Under these conditions, one molecule of MDA reacts with two molecules of TBA with the elimination of two molecules of water to yield a yellow-orange product which has characteristic fluorescence excitation and emission maxima in the range of 530 ± 5 and 555 ± 5 nm, respectively [41]. Briefly, 4×10^6 cells were mixed with 3 mL of a solution of 100 μL of KCl (0.15 μM), 100 μL of sodium dodecyl sulfate (0.28 M), 750 μL of acetic acid (3.5 mM, pH 3.5), 750 μL of TBA (55 mM), and 300 μL of distilled water. After 30–45 min of incubation at 95° in the dark, the cell mixture was cooled on ice before adding 100 μL of distilled water and 2.5 mL of butanol. After vortexing, the cell mixture was centrifuged at 1000 *g* for 20 min. The supernatant corresponding to the organic phase was collected and its fluorescence value was measured on a luminescence spectrometer (Model LS SOB, Perkin-Elmer) (excitation: 520 nm; emission: 560 nm).

2.13. Statistical methods

Statistical analyses were performed with SYSTAT software by using ANOVA. The cutoff value of significance was $P < 0.05$.

3. Results

3.1. Analysis of mitochondrial transmembrane potential ($\Delta\Psi_m$), nuclear morphology, caspase-3 activation, poly(ADP-ribose)polymerase degradation, and DNA degradation

Apoptosis is a major form of cell death characterized by a series of stereotypic morphological and biochemical features. Under the action of chemically defined molecules, especially antitumoral drugs, it seems now well understood that morphological changes associated with apoptosis are most often associated with a loss of mitochondrial transembrane potential ($\Delta\Psi_m$), caspase-3 activation, PARP degradation, and intemucleosomal DNA degradation [42,43]. These observations were confirmed in the present study performed with U937 promonocytic leukemia cells, which were treated with some pro-apoptotic molecules such as oxysterols (7β-hydroxycholesterol (50 μM, 18 hr), and 7-ketocholesterol (100 μM, 24 hr) used at concentrations near of those found in human plasmas after a reach fat meal [7]), antitumoral drugs from unrelated structures and mechanisms (VB (11 nM, 24 hr), Ara-C (50 μM, 24 hr), CHX (178 μM, 18 hr), and VP-16 (50 μM, 5 hr)), or STS (0.5 μM, 18 hr), which is an antibiotic inhibiting different isoforms of protein kinase C [22]. With these different compounds, the concentrations and the lengths of treatment were chosen in order to obtain maximal proportions of apoptotic cells. Under these conditions, the highest proportion of apoptotically dying cells characterized by condensed and/or fragmented nuclei (Fig. 1A and B) was obtained with antitumoral drugs ($60 \pm 6\%$ to $73 \pm 7\%$), and with STS ($93 \pm 3\%$) (Table 1). Under treatment with 7-ketocholesterol and 7β-hydroxycholesterol, 40 ± 2 and $45 \pm 5\%$ of apoptotic cells were found, respectively (Table 1). It is noteworthy to say that with the different pro-apoptotic molecules investigated, the mode of cell death by apoptosis was associated with the following cellular events: loss of mitochondrial transmembrane potential ($\Delta\Psi_m$) indicated by lower proportions of $DiOC_6(3)$ positive cells in treated than in untreated cells, caspase-3 activation and PARP degradation revealed both by immunocytochemistry and by Western blot analysis, and internucleosomal DNA degradation (Tables 1 and 2; Fig. 1). By immunohistochemistry, caspase-3 activation and PARP degradation were revealed in

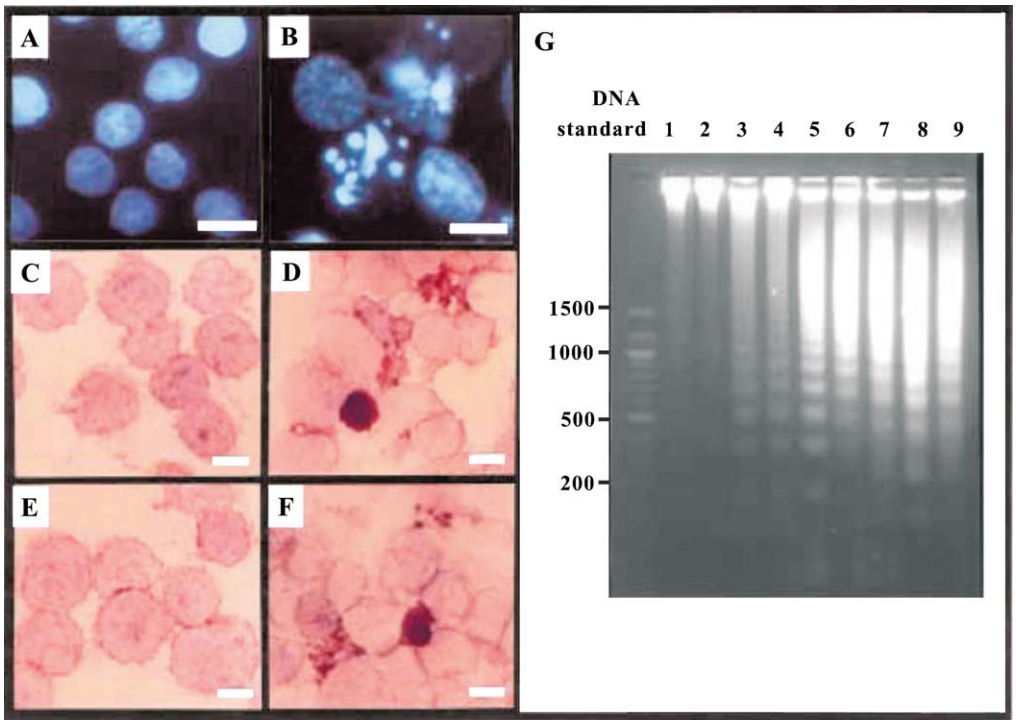

Fig. 1. Morphological, immunocytochemical and biochemical characterization of cell death. U937 cells were treated with either oxysterols oxidized at C7 (7α-hydroxycholesterol (200 μM, 24 hr), 7β-hydroxycholesterol (50 μM, 18 hr), and 7-ketocholesterol (100 μM, 24 hr)) with antitumoral drugs (VB (11 nM, 24 hr), Ara-C (50 μM, 24 hr), CHX (178 μM, 18 hr), and VP-16 (50 μM, 5 hr)), or with STS (0.5 μM, 18 hr). Apoptotic cells were identified after nuclei staining with Hoechst 33342. Caspase-3 activation and PARP degradation were determined by immunohistochemistry on cell deposits, and the DNA fragmentation pattern was characterized by electrophoresis on agarose gel. Nuclear morphology of untreated cells (A) and 7β-hydroxycholesterol-treated cells (B). Immunocytochemical analysis of caspase-3 activation on untreated cells (C) and 7β-hydroxycholesterol-treated cells (D), as well as PARP degradation on untreated cells (E) and 7β-hydroxycholesterol-treated cells (F). In each case the scale bar is 10 μm. G: analysis of DNA fragmentation by electrophoresis on agarose gel (1: untreated cells; 2: 7α-hydroxycholesterol; 3: 7β-hydroxycholesterol; 4: 7-ketocholesterol; 5: VB; 6: Ara-C; 7: CHX; 8: VP-16; 9: STS): no DNA fragmentation was observed in untreated cells, whereas internucleosomal DNA fragmentation patterns were found with all compounds investigated, except 7α-hydroxycholesterol. Data shown are representative of three independent experiments.

some cells by intense brown stainings which were not present in untreated cells (Fig. 1C–F). By Western blot, inactive caspase-3 (32 kDa) as well as its processed form consisting of large (17 kDa) and small (12 kDa) subunits which associate to form an active enzyme were visualized (Table 2). Subsequent cleavage of PARP (115 kDa) by activated caspase-3 was revealed by the presence of the 85 kDa characteristic proteolytic degradation fragment of

Table 1
Quantification and characterization of apoptosis induced by oxysterols (7α-, 7β-hydroxycholesterol, and 7-ketocholesterol), by antitumoral drugs (VB, Ara-C, CHX, and VP-16) and by STS with the use of morphological and biochemical criteria

	Percent of depolarized cells	Percent of apoptotic cells	Caspase-3 activation	PARP degradation	Internucleosomal DNA fragmentation
Control	7 ± 2	3 ± 1	−	−	−
7α-Hydroxycholesterol (200 μM, 24 hr)	6 ± 1*	4 ± 1*	−	−	−
7β-Hydroxycholesterol (50 μM, 18 hr)	70 ± 5*	45 ± 5*	+	+	+
7-Ketocholesterol (100 μM, 24 hr)	60 ± 4*	30 ± 5*	+	+	+
VB (11 nM, 24 hr)	85 ± 7*	73 ± 7*	+	+	+
Ara-C (50 μM, 24 hr)	80 ± 6*	60 ± 6*	+	+	+
CHX (178 μM, 18 hr)	82 ± 5*	64 ± 5*	+	+	+
VP-16 (50 μM, 5 hr)	92 ± 5*	66 ± 3*	+	+	+
STS (0.5 μM, 18 hr)	82 ± 6*	93 ± 3*	+	+	+

Percent of depolarized cells corresponding to cells characterized by a loss of mitochondrial transmembrane potential ($\Delta\Psi_m$) were determined by flow cytometry after staining with $DiOC_6(3)$. Percent of apoptotic cells (with fragmented and/or condensed nuclei) was determined after staining with Hoechst 33342, caspase-3 activation and PARP degradation were evaluated by immunocytochemistry, and internucleosomal DNA fragmentation was characterized on agarose gel. Data represent three independent experiments realized in triplicate. (*) Statistically significant differences ($P < 0.05$) between control (untreated cells) and treated cells.

Table 2
Effects of oxysterols (7α-, 7β-hydroxycholesterol and 7-ketocholesterol), antitumoral drugs (VB, Ara-C, CHX, VP-16) and STS on caspase-3 activation and poly(ADP-ribose)polymerase degradation

Treatments

	Control (24 h)	7α (200 μM, 24 h)	7β (50 μM, 18 h)	7-keto (100 μM, 24 h)	VB (11 nM, 24 h)	Ara-C (50 μM, 24 h)	CHX (178 μM, 18 h)	VP-16 (50 μM, 5 h)	STS (0.5 μM, 18 h)	
caspase-3 activity (pMol AMC/min)	9 ± 2	9 ± 2	35 ± 5 *	100 ± 5 *	177 ± 8 *	137 ± 7 *	69 ± 2 *	172 ± 37 *	133 ± 20 *	
caspase-3										32 kD 17 kD 12 kD
PARP										115 kD 85 kD

Caspase-3 activity was analyzed by fluorogenic assays. Caspase-3 cleavage and poly(ADP-ribose)polymerase degradation were investigated by Western blot. Data corresponding to caspase-3 activity represent three independent experiments performed in triplicate. Western blot data are representative of three independent experiments. (*) Statistically significant differences ($P < 0.05$) between control (untreated cells) and treated cells.

PARP (Table 2). In addition, under treatment with 7-ketocholesterol and 7β-hydroxycholesterol as well as with the different pro-apoptotic chemicals used, caspase-3 activity was significantly ($P < 0.05$) enhanced comparatively to untreated cells (Table 2). In agreement with our previous studies [17], no sign of apoptosis was seen after treatment with 7α-hydroxycholesterol (Tables 1 and 2).

3.2. Involvement of oxidative stress in chemical-induced apoptosis

Our data underline that some morphological and biochemical characteristics of apoptosis (loss of mitochondrial transembrane potential, occurrence of cells with fragmented and/or condensed nuclei, caspase-3 activation, PARP degradation, and internucleosomal DNA degradation) are similar despite the diversity of chemical molecules capable of inducing apoptosis. However, numerous investigations suggest important differences in the ability of pro-apoptotic compounds to trigger oxidative stress [44,45]. Therefore, this led us to investigate superoxide anion ($O_2^{\bullet -}$) production and lipid peroxidation on U937 cells treated with either oxysterols (7β-hydroxycholesterol, 7-ketocholesterol), antitumoral drugs (VB, Ara-C, CHX, VP-16), or STS at two times of treatment: one before and one after the loss of mitochondrial transembrane potential. Overproduction of $O_2^{\bullet -}$ was quantified by flow cytometry after staining with HE. Before the loss of mitochondrial transembrane potential, slight overproduction of $O_2^{\bullet -}$ and slight lipid peroxidation were observed with the different antitumoral drugs investigated (VB (11 nM, 2 hr), Ara-C (50 μM, 2 hr), CHX (178 μM, 2 hr), VP-16 (0.5 μM, 1 hr) as well as with STS (0.5 μM, 2 hr). Indeed, with these different molecules, the proportions of HE positive cells were slightly but significantly ($P < 0.05$) higher than in untreated cells (Table 3, Fig. 2). Of note, under treatment with 7β-hydroxycholesterol (50 μM, 10 hr) and 7-ketocholesterol (100 μM, 10 hr), important overproductions of $O_2^{\bullet -}$ indicated by the mean fluorescence of HE positive cells were observed among a high proportion of cells (7β-hydroxycholesterol: 41 ± 5% 7-ketocholesterol: 70 ± 3%) (Table 3, Fig. 2). After the loss of mitochondrial transmembrane potential, with 7β-hydroxycholesterol (50 μM, 18 hr) and 7-ketocholesterol (100 μM, 24 hr), the proportions and the means of fluorescence of HE positive cells were similar or higher than those found before the loss of mitochondrial transmembrane potential (Table 3). Under treatment with antitumoral drugs, heterogeneous results were obtained. Thus, with VP-16 (50 μM, 5 hr) overproduction of $O_2^{\bullet -}$ was in the same range than those measured at 1 hr, and with Ara-C (50 μM, 24 hr) overproduction of $O_2^{\bullet -}$ was moderately but significantly ($P < 0.05$) increased. However, with VB (11 nM, 24 hr), and CHX (178 μM, 24 hr), the proportions of cells overproducing $O_2^{\bullet -}$ as well as the mean fluorescence intensity of HE positive cells were strongly enhanced but the levels of $O_2^{\bullet -}$ overproduction as well as the proportions of cells overproducing $O_2^{\bullet -}$ were lower than those obtained under treatment with 7β-hydroxycholesterol and 7-ketocholesterol. With STS

Table 3
Evaluation of the protective effects of Vit E on oxidative stress (surproduction of superoxide anions, lipid peroxidation)

Treatments	Percent of depolarized cells	Percent of HE positive cells	Mean fluorescence (HE positive cells)	MDA (nmol/10^9 cells)	Percent of MDC positive cells	Percent of apoptotic cells
Control 2 hr/10 hr/24 hr	6 ± 2/6 ± 1/7 ± 2	5 ± 1/5 ± 2/6 ± 2	ND	16 ± 1/18 ± 2/20 ± 3	2 ± 1/3 ± 1/4 ± 1	3 ± 1/3 ± 1/3 ± 1
Vit E (100 μM) 2 hr/10 hr/24 hr	7 ± 4/7 ± 2/9 ± 4	5 ± 2/5 ± 1/6 ± 3	ND	13 ± 3/12 ± 1/18 ± 3	2 ± 1/2 ± 1/2 ± 1	4 ± 2/4 ± l/5 ± 1
7α (200 μM) 10 hr/24 hr	6 ± 3/6 ± 1	5 ± 1/6 ± 2	ND	14 ± 3/15 ± 4	2 ± 1/3 ± 1	4 ± 2/4 ± 1
7β (50 μM) 10 hr/18 hr	10 ± 3/70 ± 5^*	41 ± 5^*/57 ± 2^*	23 ± 2/40 ± 5	33 ± 2^*/45 ± 8^*	51 ± 7/77 ± 5	6 ± 1^*/45 ± 5^*
7β + Vit E 10 hr/18 hr	6 ± 4/55 ± 5^{**}	35 ± 6/45 ± 2^{**}	18 ± 1/30 ± 4^{**}	21 ± 7^{**}/30 ± 6^{**}	38 ± 4^{**}/55 ± 5^{**}	5 ± 2/25 ± 5^{**}
7-Keto (100 μM) 10 hr/24 hr	8 ± 4/60 ± 4^*	70 ± 3^*/65 ± 5^*	23 ± 3/35 ± 4	30 ± 1^*/106 ± 15^*	40 ± 3^*/83 ± 6^*	5 ± 2/30 ± 5^*
7-Keto + Vit E 10 hr/24 hr	8 ± 2/40 ± 2^{**}	33 ± 5^{**}/50 ± 5^{**}	18 ± 1^{**}/25 ± 3^{**}	20 ± 1^{**}/90 ± 10^{**}	28 ± 2^{**}/42 ± 2^{**}	6 ± 1/13 ± 4^{**}
VB (11 nM) 2 hr/24 hr	9 ± 4/85 ± 7^*	12 ± 1^*/36 ± 6^*	21 ± 6^*/30 ± 1^*	28 ± 2^*/122 ± 18^*	3 ± 1/3 ± 1	5 ± 1/73 ± 7^*
VB + Vit E 2 hr/24 hr	9 ± 4/28 ± 2^{**}	4 ± 2^{**}/11 ± 2^{**}	22 ± 6/28 ± 1^{**}	20 ± 3^*/91 ± 24^*	2 ± 1/3 ± 1	4 ± 2/28 ± 10^{**}
Ara-C (50 μM) 2 hr/24 hr	10 ± 5^*/80 ± 6^*	9 ± 3^*/14 ± 4^*	16 ± 1/22 ± 5	25 ± 3^*/100 ± 14^*	4 ± 1/3 ± 1	4 ± 2/60 ± 6^*
Ara-C + Vit E 2 hr/24 hr	11 ± 5/75 ± 8	8 ± 2/10 ± 6	15 ± 1/20 ± 5	20 ± 3/90 ± 13	3 ± 1/3 ± 1	5 ± 2/55 ± 8
CHX (178 μM) 2 hr/24 hr	10 ± 2/82 ± 5^*	9 ± 5^*/34 ± 11^*	17 ± 1^*/28 ± 2^*	24 ± 6^*/126 ± 10^*	4 ± 1/3 ± 1	4 ± 2/64 ± 5^*
CHX + Vit E 2 hr/24 hr	10 ± 3/78 ± 3	5 ± 4/28 ± 8	17 ± 1/25 ± 3	20 ± 3/95 ± 25	4 ± 2/3 ± 2	3 ± 1/57 ± 3
VP-16 (50 μM) 1 hr/24 hr	6 ± 2/92 ± 5^*	11 ± 2^*/15 ± 2^*	16 ± 1^*/23 ± 5^*	20 ± 5/27 ± 5	4 ± 1/3 ± 1	6 ± 2/66 ± 3^*
VP-16 + Vit E 1 hr/5 hr	6 ± 1/88 ± 3	10 ± 5/12 ± 3	15 ± 3/20 ± 5	23 ± 5/23 ± 5	3 ± 1/3 ± 1	6 ± 3/60 ± 5
STS (0.5 μM) 2 hr/18 hr	9 ± 3/82 ± 6^*	9 ± 2^*/32 ± 5^*	16 ± 1^*/26 ± 4^*	22 ± 3/86 ± 4	4 ± 1/3 ± 1	5 ± 2/93 ± 3^*
STS + Vit E 2 hr/18 hr	10 ± 4/25 ± 7^{**}	6 ± 1^{**}/22 ± 5^{**}	16 ± 2/22 ± 1^{**}	16 ± 3/52 ± 5^{**}	3 ± 2/3 ± 1	4 ± 1/12 ± 4^{**}

Data represent three independent experiments performed in triplicate. Flow cytometry was used to determine the percentages of depolarized cells, of cells overproducing superoxide anions, and of cells with autophagic vacuoles determined after staining with $DiOC_6(3)$, hydroethidine (HE) and monodansylcadaverine (MDC), respectively. The percentages of apoptotic cells were determined by fluorescence microscopy after nuclei staining with Hoechst 33342. Lipid peroxidation was measured by fluorometric quantification of malondialdehyde (MDA). When the proportions of HE positive cells were similar than in control (untreated cells), mean fluorescence of positive cells was difficult to estimate and was therefore not determined (ND). (∗) Statistically significant differences ($P < 0.05$) between control (untreated cells) and treated cells. (∗∗) Statistically significant differences ($P < 0.05$) between treated cells and treated cells pws Vit E.

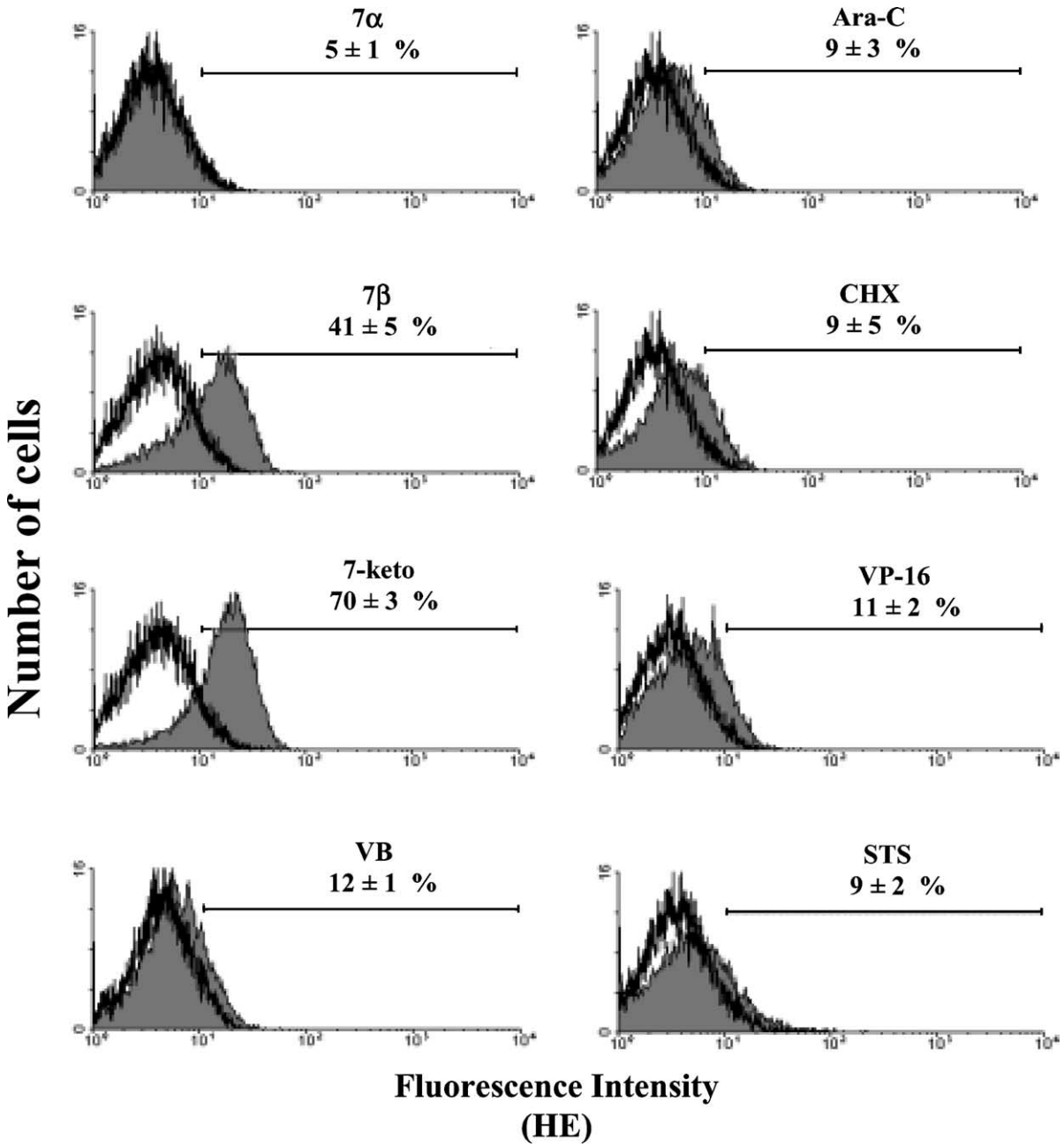

Fig. 2. Effects of oxysterols, antitumoral drugs, and STS on the overproduction of superoxide anions. Flow cytometric analysis of the effects of oxysterols oxidized at C7 (7α-hydroxycholesterol (200 μM, 10 hr), 7β-hydroxycholesterol (50 μM, 10 hr), and 7-ketocholesterol (100 μM, 10 hr)), antitumoral drugs (VB (11 nM, 2 hr), Ara-C (50 μM, 2 hr), CHX (178 μM, 2 hr), and VP-16 (50 μM, 1 hr)), and STS (0.5 μM, 2 hr) on the overproduction of superoxide anion ($O_2^{\bullet -}$) measured by flow cytometry after staining with hydroethidine (HE) before the loss of mitochondrial transmembrane potential. The fluorescence associated with HE was measured on a logarithmic scale of fluorescence, and 5000 cells were analyzed for each assay. Unshaded histograms: fluorescence associated with HE in untreated cells; shaded histograms: fluorescence associated with HE in 7α-hydroxycholesterol-treated cells (7α), 7β-hydroxycholesterol-treated cells (7β), 7-ketocholesterol-treated cells (7-keto), VB-treated cells, Ara-C-treated cells, CHX-treated cells, STS-treated cells, and VP-16-treated cells (for each shaded histogram, the proportion of cells overproducing $O_2^{\bullet -}$ is indicated). Data shown are representative of three independent experiments realized in triplicate.

(0.5 μM, 18 hr), the proportion of cells overproducing $O_2^{\bullet -}$ as well as the level of $O_2^{\bullet -}$ production were in the range of those obtained with VB (11 nM, 24 hr) and CHX (178 μM, 24 hr) (Table 3).

As $O_2^{\bullet -}$ represents only one type of ROS susceptible to being overproduced during apoptosis, we also quantified MDA in control and treated cells. Indeed, MDA constitutes an endproduct of lipid peroxidation which can be induced by various ROS [30]. In those conditions, low proportions of HE positive cells were associated with low levels of MDA production, whereas high proportions of HE positive cells were associated with high MDA levels (Table 3). Under treatment with 7α-hydroxycholesterol (200 M), no loss of mitochondrial transmembrane potential, no

overproduction of $O_2^{\bullet -}$ and no lipid peroxidation were detected at the different times investigated (Table 3).

As Vit E has been described to protect against atherosclerosis [36], and as we previously reported that Vit E was capable to counteract 7-ketocholesterol-induced apoptosis [20], the ability of this antioxidant to block the generation of free radicals and to inhibit lipid peroxidation before and/or after the loss of mitochondrial transmembrane potential was investigated. Noteworthy, statistically significant ($P < 0.05$) protective effects of Vit E against 7β-hydroxycholesterol, 7-ketocholesterol-, VB-, and STS-induced apoptosis were observed: loss of mitochondrial transmembrane potential, overproduction of $O_2^{\bullet -}$ and lipid peroxidation were reduced as well as the proportions of cells

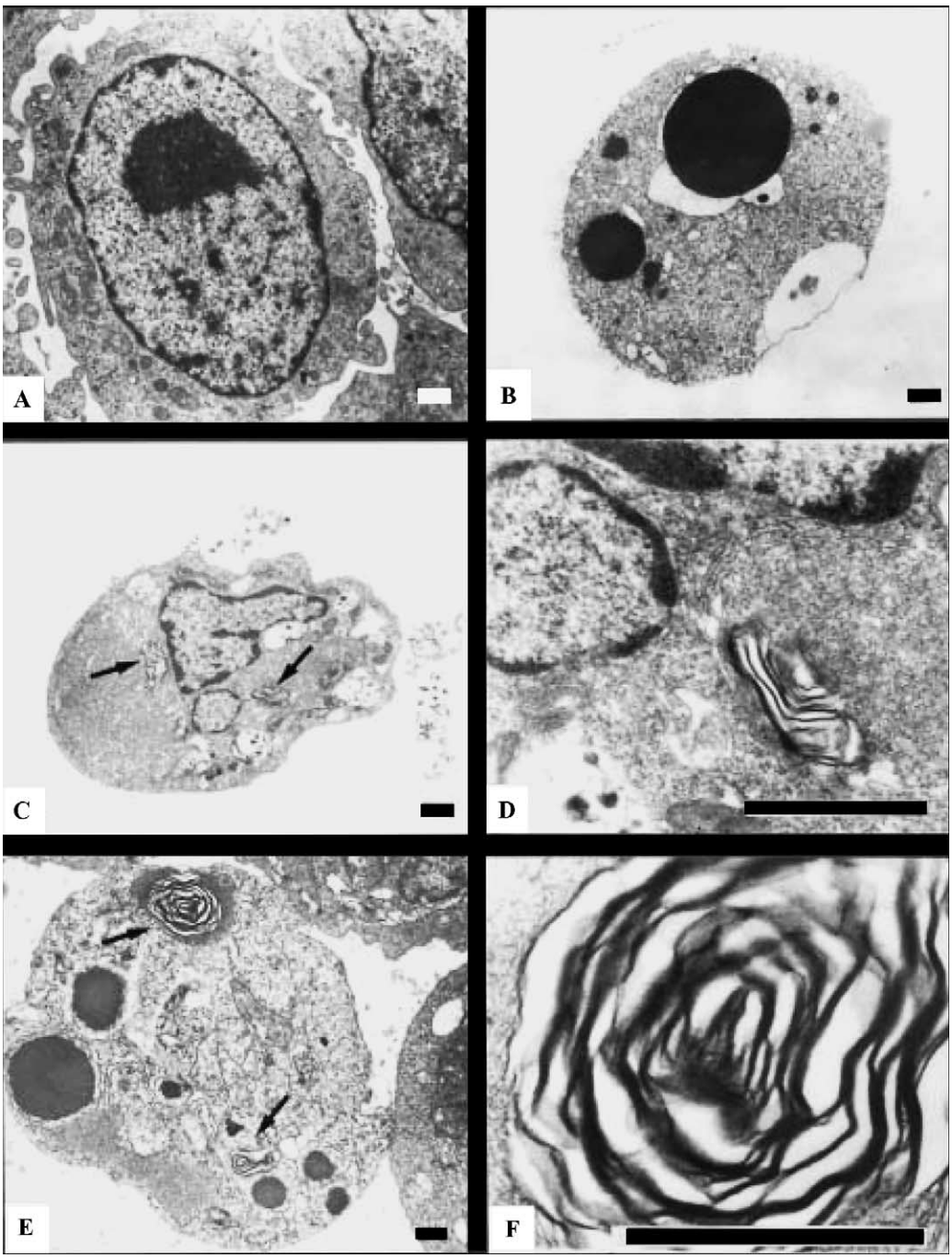

Fig. 3. Electron microscopic detection of myelin figures in apoptotic cells obtained after treatment with 7β-hydroxycholesterol and 7-ketocholesterol. Various aspects of myelin figures evocating autophagic vacuoles were observed in apoptotic U937 cells obtained after treatment with 7β-hydroxycholesterol (50 μM, 18 hr) (C and D) or 7-ketocholesterol (100 μM, 24 hr) (E and F). High magnification of myelin figures (D–F) indicated by arrows in apoptotic cells obtained after treatment with 7β-hydroxycholesterol (C) or 7-ketocholesterol (E). Myelin figures were never observed in untreated cells (A), and in VB (11 nM, 24 hr) treated cells (B). In each case, the scale bar is 1 μm.

with fragmented and/or condensed nuclei which are characteristic of apoptotic cells (Table 3). However, slight but not significant protective effects of Vit E were found against, Ara-C-, CHX-, and VP-16-induced apoptosis (Table 3).

Thus, among the different pro-apoptotic agents investigated, 7β-hydroxycholesterol and 7-ketocholesterol were the most potent inducers of oxidative stress (overproduction of $O_2^{\bullet -}$ and lipid peroxidation), and the cytotoxic effects of these oxysterols were impaired by Vit E.

3.3. Formation of myelin figures during 7β-hydroxycholesterol and 7-ketocholesterol-induced apoptosis

As myelin figures were previously observed by transmission electron microscopy on human vascular endothelial cells treated with 7-ketocholesterol [32], ultrastructural experiments were performed to determine whether these abnormal cellular structures could constitute ultrastructural markers of oxysterol-induced apoptosis, or of apoptosis associated with the overproduction of ROS. In untreated cells (Fig. 3A), as well as under treatment with STS (0.5 μM) and the antitumoral drugs (VB (11 nM), Ara-C (50 μM), CHX (178 μM), and VP-16 (50 μM)), myelin figures were never observed either before or after the loss of mitochondrial transmembrane potential (Table 3). So, after treatment with VB (11 nM, 24 hr), myelin figures were never detected, whereas this compound induced the highest proportion of HE positive cells compared to other antitumoral drugs and to STS (Table 3, Fig. 3B). Interestingly, with 7β-hydroxycholesterol (50 μM, 18 hr) and 7-ketocholesterol (100 μM, 24 hr), myelin figures of various sizes and shapes were detected in the cytoplasm of apoptotically dying cells taken at different stages of apoptosis. Thus, under treatment with these oxysterols, myelin figures were observed in early apoptotic cells characterized by perinuclear localization of the chromatin (Fig. 3C and D), as well as in late apoptotic cells with fragmented and/or condensed nuclei and condensed chromatin (Fig. 3E and F). The sizes of these myelin figures were generally larger in late, rather than in early, apoptotic cells (Fig. 3D–F). As multilamellar bodies, ultrastructurally identical to myelin figures have been shown to correspond to autophagic vacuoles [31], untreated as well as oxysterols-, antitumoral drugs-, and STS-treated cells were stained with MDC, a lysosomotropic agent which specifically stains autophagic vacuoles appearing as large green spots in the cyoplasm under UV light excitation [33,34]. In those conditions, fluorescent cells (MDC positive cells) were only observed under treatment with 7-ketocholesterol and 7β-hydroxycholesterol both before and after the loss of mitochondrial transmembrane potential (Fig. 4), and the percentages of MDC positive cells were significantly ($P < 0.05$) decreased by Vit E (Table 3).

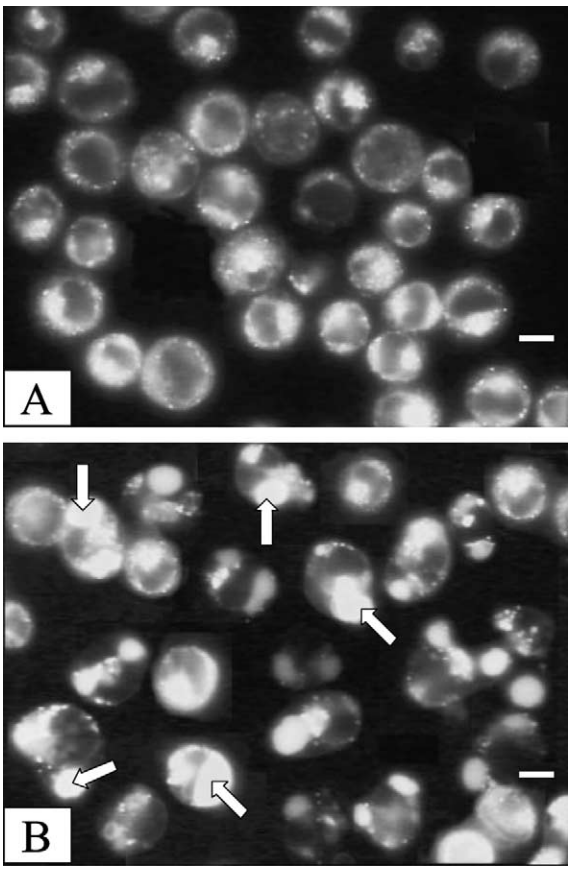

Fig. 4. Labeling of 7β-hydroxycholesterol and 7-ketocholesterol-treated cells by monodansylcadaverine. Staining patterns obtained with monodansylcadaverine (MDC) of untreated (24 hr) (A) and 7-ketocholesterol (100 μM, 24 hr) treated (B) U937 cells. Cellular structures stained by MDC (corresponding probably to autophagic vacuoles) are indicated by arrows. Similar aspects than those obtained under treatment with 7-ketocholesterol were found with 7-hydroxycholesterol. In each case, the scale bar is 10 μm.

Since myelin figures, evocating autophagic vacuoles, were only found by transmission electron microscopy under treatment with 7β-hydroxycholesterol and 7-ketocholesterol, and as MDC only stains 7β-hydroxycholesterol and 7-ketocholesterol-treated cells, our data suggest that myelin figures could correspond to autophagic vacuoles. In addition, since myelin figures are not detected in VB- and STS-treated cells whereas these molecules strongly stimulate late oxidative stress, the present data favor the hypothesis that these abnormal cellular structures could constitute reliable markers of oxysterol-induced apoptosis rather than apoptosis associated with late oxidative stress.

4. Discussion

ROS are not only toxic side-products of oxygen metabolism in mammalian cells, but they also have important normal physiological functions, including antimicrobial killing, regulation of cellular proliferation and growth,

and regulation of vascular tone [46]. To date, increasing evidence provides support that apoptosis and oxidative stress are closely linked phenomena and are implicated in the pathophysiology of some chronic diseases including atherosclerosis [46–48]. So, 7β-hydroxycholesterol and 7-ketocholesterol which are major components of oxidized low density lipoproteins involved in the formation of atherosclerotic lesions [49], and which are present at increased concentrations in atheromatous plaques [9–11], could play critical roles in the initiation and development of atherosclerosis. Indeed, 7β-hydroxycholesterol and 7-ketocholesterol have been shown to induce apoptosis on a wide number of cells, including those of the vascular wall [15], and previous investigations in our laboratory suggest that 7-ketocholesterol enhances ROS production [19], especially superoxide anion ($O_2^{\bullet -}$) production [20]. To specify the relationship between apoptosis and oxidative stress, it was therefore of interest to investigate these phenomena on 7β-hydroxycholesterol and 7-ketocholesterol-treated cells in comparison with other potent inducers of apoptosis, such as antitumoral drugs (VB, Ara-C, CHX, and VP-16), and STS. Interestingly, the present *in vitro* study performed on U937 cells shows that the most important enhancements of $O_2^{\bullet -}$ production are obtained under treatment with 7β-hydroxycholesterol and 7-ketocholesterol, whereas important variations were detected with the other pro-apoptotic chemicals (VB, Ara-C, CHX, VP-16, and STS) investigated. Therefore, 7β-hydroxycholesterol and 7-ketocholesterol, which are undetectable or present at low level in normal human arteries but significantly enhanced in atherosclerotic lesions [9–11], could stimulate ROS production *in vivo* and contribute to the inflammatory process, which is a main component of atherosclerosis. In addition, by electron microscopy, myelin figures were only observed under treatment with 7β-hydroxycholesterol and 7-ketocholesterol, suggesting that these abnormal ultrastructural features could constitute suitable markers of oxysterol-induced apoptosis.

Thus, in agreement with our previous studies [17], 7β-hydroxycholesterol and 7-ketocholesterol-induced apoptosis is accompanied by the appearance of cells with fragmented and/or condensed nuclei, caspase-3 activation, PARP degradation, and intemucleosomal DNA degradation. Similar features were also observed with the antitumoral drugs investigated (VB, Ara-C, CHX, and VP-16) and with STS. Thus, while the initial signal for apoptosis varies with all chemicals investigated [43], cell death by apoptosis appears to converge towards highly conserved sequences of events. Therefore, according to the diversity of the signals and of the metabolic pathways capable of triggering apoptosis, it seems more and more crucial to characterize apoptosis by additional criteria, especially in terms of overproduction of radical oxygen species (ROS) since this event, which can have some physiopathological repercussions, has been suggested either as a part of the signal transduction pathway in apoptotically dying cells or as a consequence of cell death by apoptosis [44,45]. Among the different molecules studied, the present work clearly demonstrates that the highest $O_2^{\bullet -}$ overproduction was obtained with oxysterols oxidized at C7 (except 7α-hydroxycholesterol, which was also not pro-apoptotic). Such data, mainly those obtained with 7β-hydroxycholesterol, are in agreement with those reported by other investigators [50,51] while apparent discrepancy results are obtained with 7-ketocholesterol [51]. However, such differences concerning the overproduction of ROS in response to treatment of U937 cells with 7-ketocholesterol are not contradictory since this oxysterol was only used at 30 μM by O'Callaghan and coworkers instead of 100 μM in the present investigation. Noteworthy, with the other chemicals studied, an important variability was found. Thus, the highest stimulations of $O_2^{\bullet -}$ overproduction were obtained with VB and STS, and the lowest with Ara-C, CHX, and VP-16. As $O_2^{\bullet -}$ represents only one type of ROS susceptible to be overproduced during apoptosis, lipid peroxidation damage, which can be induced by various ROS, was also measured in apoptotic cells by a fluorimetric reaction with TBA to quantify MDA, an end-product of lipid peroxidation [30]. Under these conditions, the most important lipid peroxidation processes were found with oxysterols and overproduction of $O_2^{\bullet -}$ was correlated with enhanced lipid peroxidation. Taken together, our data provide support that during apoptosis, the intensity of oxidative stress depends on the pro-apoptotic molecules considered. In addition, as an important stimulation of oxidative processes ($O_2^{\bullet -}$ overproduction and lipid peroxidation) was detected both before and after the loss of mitochondrial transmembrane potential under treatment with 7β-hydroxycholesterol and 7-ketocholesterol, but mainly after the loss of mitochondrial transmembrane potential under treatment with antitumoral drugs (VB, Ara-C, CHX, and VP-16) and STS, our observations lead us to hypothesize that late $O_2^{\bullet -}$ overproduction probably results of mitochondrial dysfunctions [52,53] whereas early $O_2^{\bullet -}$ overproduction could be the consequence of a rapid disruption of the redox equilibrium. Indeed, since viable cells maintain a redox equilibrium by balancing cytoplasmic levels of oxidants and antioxidants, the early important stimulation of oxidative stress observed under treatment with 7β-hydroxycholesterol and 7-ketocholesterol could be explained by the simultaneous capability of these oxysterols to strongly stimulate the production of ROS [19,20], and to induce a rapid decreased of reduced glutathione (GSH) [16,19,50]. We can also not exclude that 7β-hydroxycholesterol and 7-ketocholesterol could rapidly activate some enzymes involved in the generation of $O_2^{\bullet -}$ such as hypoxanthine/xanthine oxidase, lipoxygenase, cyclooxygenase or NADPH-oxidase playing a critical role in several early steps leading towards the development of atherosclerosis [54,55]. Indeed, enrichment of mouse peritoneal macrophages with 7-ketocholesterol and 7β-hydroxycholesterol resulted in a dose-dependent

increase in NADPH-oxidase activity associated with an enhancement of $O_2^{\bullet -}$ release [56]. So, as 7β-hydroxycholesterol and 7-ketocholesterol are major components of oxidized LDL (oxLDL), and as oxLDL-induced apoptosis has been described to generate ROS [57], it is more and more tempting to speculate that oxLDL, which are known to accumulate in atherosclerotic plaques, could exert their proinflammatory effects, at least in part, *via* these oxysterols.

To precise the *in vivo* involvement of oxysterols in cell damage and in the inflammatory processes throughout the different stages of atherosclerosis [58], it is of interest to have specific markers associated with the side effects of these molecules. As previous studies in our laboratory performed using transmission electron microscopy on human vascular endothelial cells treated with 7-ketocholesterol revealed formations of multilamellar, onion-like structures (named myelin figures) in the cytoplasm of apoptotic cells [32], we asked whether these abnormal ultrastructural figures, corresponding probably to autophagic vacuoles according to positive staining obtained with MDC [59–61], could constitute specific markers of oxysterol-induced cell death. It is particularly noteworthy to observe that myelin figures are only present in apoptotic cells obtained under treatment with 7β-hydroxycholesterol and 7-ketocholesterol, and that they can be detected at both early and late stages of apoptosis before and after the loss of mitochondrial transmembrane potential. Therefore, this observation strongly suggests that these myelin figures could constitute convenient markers of 7β-hydroxycholesterol and 7-ketocholesterol-induced apoptosis, which could further permit the determination of the *in vivo* role played by these oxysterols at various stages of the formation of atherosclerotic plaque. In addition, as myelin figures were not detected in VB- and STS-treated cells which strongly stimulate oxidative stress mainly after the loss of mitochondrial transmembrane potential, whereas they were present in 7β-hydroxycholesterol and 7-ketocholesterol-treated cells which enhance oxidative stress both before and after the decrease of mitochondrial transmembrane potential, the present data suggest that these abnormal cellular structures could be associated with early oxidative stress. This later hypothesis was reinforced by the use of Vit E. Indeed, when the cells were simultaneously treated by 7β-hydroxycholesterol and 7-ketocholesterol in the presence of Vit E, early oxidative stress was strongly reduced as well as the proportions of MDC positive cells and of apoptotic cells. With antitumoral drugs and STS, data obtained with Vit E also permit to precise the roles of ROS in the mechanisms of cell death induced by these pro-apoptotic chemicals. Thus, the ability of Vit E to impair VB- and STS-induced apoptosis favors the hypothesis that ROS are involved in metabolic pathways leading to cell death. In the contrary, the inability of Vit E to counteract Ara-C- and CHX-induced apoptosis rather suggests that the occurrence of oxidative stress observed under treatment with these molecules is the consequence of late secondary processes occurring after a point of non-return. The lack of protective effect of Vit E on VP-16-induced apoptosis brings also new insights on the mechanism of this antitumoral drug, and leads us to suppose that the slight increase of oxidative stress does not contribute to trigger apoptosis whereas the decrease of intracellular GSH observed under treatment with VP-16 [62], and also found with numerous pro-apoptotic molecules [63], probably plays critical roles in the regulation of cell death. This later hypothesis is in agreement with previous investigations which reported that GSH and *N*-acetylcysteine (NAC), a precursor of GSH, were capable to prevent VP-16-induced apoptosis [19,64].

In conclusion, the present study has demonstrated that apoptosis can occur either with low or important oxidative stress, and that the enhancement of $O_2^{\bullet -}$ production and lipid peroxidation varied according to the pro-apoptotic agent considered. Thus, among the different molecules investigated, whereas 7β-hydroxycholesterol and 7-ketocholesterol were not the most potent inducers of apoptosis, they were the most efficient compounds capable of strongly stimulating $O_2^{\bullet -}$ production and lipid peroxidation as well as the formation of myelin figures evocating autophagic vacuoles, both before and after the loss of mitochondrial transmembrane potential. Since 7β-hydroxycholesterol and 7-ketocholesterol induce similar features of cell death on U937 cells and on the cells of the vascular wall (endothelial cells, smooth muscle cells) [65,66] contributes to reinforce the hypothesis that these oxysterols may be responsible for the formation of initial lesions in the vascular wall and to their developpment. Therefore, 7β-hydroxycholesterol and 7-ketocholesterol, which are found at increased levels in the plasma and in the arterial wall of hypercholesterolemic patients [8–11], could contribute to the initiation and progression of vascular lesions by their simultaneous ability to promote cell death involving apoptotic and autophagic processes, and to initiate inflammatory reactions. So, it is more and more tempting to speculate that 7β-hydroxycholesterol and 7-ketocholesterol could constitute an essential molecular link between hypercholesterolemia, inflammatory processes, and atherosclerosis.

Acknowledgments

This work was supported by the Université de Bourgogne, the Conseil Regional de Bourgogne, the Institut National de la Santé et de la Recherche Medicale (Inserm), the Fondation pour Ia Recherche Me dicale (FRM), and the Fondation de France. We thank the Centre de Microscopie Appliqué à la Biologie (Université de Bourgogne, Dijon, France) for the observations by transmission electron microscopy. The authors are also indebted to Jonathan Ewing for reviewing the English version of this manuscript.

References

[1] Yuan YV, Kitts DD, Clodin DV. Influence of dietary cholesterol and fat source on atherosclerosis in the Japanese quail (*Cotumix japonica*). Br J Nutr 1997;78:993–1014.

[2] Ktari L, Blond A, Guyot M. 16β-Hydroxy-5α-cholestane-3,6-dione, a novel cytotoxic oxysterol from the red alga *Jania rubens*. Biorg Med Chem Lett 2000;10:2563–5.

[3] Schroepfer GJ. Oxysterols: modulators of cholesterol metabolism and other processes. Physiol Rev 2000;80:361–554.

[4] Smith LL. Cholesterol autoxidation. Chem Phys Lipids 1987;44:87–125.

[5] Russell DW. Oxysterol biosynthetic enzymes. Biochim Biophys Acta 2000;1529:126–35.

[6] Smith LL. Another cholesterol hypothesis: cholesterol as antioxidant. Free Radic Biol Med 1991;11:47–61.

[7] Emanuel HA, Hassel CA, Addis PB, Bergmann SD, Zavoral JH. Plasma cholesterol oxidation products (oxysterols) in human subjects fed a meal rich in oxysterols. J Food Sci 1991;56:843–7.

[8] Zhou Q, Wasowicz E, Handler B, Fleischer L, Kummerow FA. An excess concentration of oxysterols in the plasma is cytotoxic to cultured endothelial cells. Atherosclerosis 2000;149:191–7.

[9] Brown AJ, Leong SL, Dean R, Jessup W. 7-Hydroperoxycholesterol and its product in oxidized low-density lipoprotein and human atherosclerotic plaque. J Lipid Res 1997;38:1730–45.

[10] Vaya J, Aviram M, Mahmod S, Hayek T, Grenadir F, Hoffman A, Milo S. Selective distribution of oxysterols in atherosclerotic lesions and human plasma lipoproteins. Free Rad Res 2001;34:485–97.

[11] Garcia-Cruset S, Carpenter KL, Guardiola F, Stein BK, Mitchinson MJ. Oxysterol profiles of normal human arteries, fatty streaks and advanced lesions. Free Rad Res 2001;35:31–41.

[12] Brown AJ, Jessup W. Oxysterols and atherosclerosis. Atherosclerosis 1999;142:1–28.

[13] Lyons NM, Woods JA, O'Brien NM. α-Tocopherol, but not γ-tocopherol inhibits 7β-hydroxycholesterol-induced apoptosis in human U937 cells. Free Rad Res 2001;35:329–39.

[14] Aupeix K, Weltin D, Mejia JE, Christ M, Marchal J, Freyssinet JM, Bischoff P. Oxysterol-induced apoptosis in human monocytic cell lines. Immunobiology 1995;194:415–8.

[15] Lizard G, Monier S, Cordelet C, Gesquière L, Deckert V, Gueldry S, Lagrost L, Gambert L. Characterization and comparison of the mode of cell death, apoptosis versus necrosis, induced by 7β-hydroxycholesterol and 7-ketocholesterol in the cells of the vascular wall. Arterioscler Tromb Vasc Biol 1999;19:1190–200.

[16] O'Callaghan YC, Woods JA, O'Brien NM. Limitation of the single-cell gel electrophoresis assay to monitor apoptosis in U937 and HepG2 cells exposed to 7β-hydroxycholesterol. Biochem Pharm 2001;61:1217–26.

[17] Miguet C, Monier S, Bettaieb A, Athias A, Bessède O, Laubriet A, Lemaire S, Néel D, Gambert P, Lizard G. Ceramide generation occuring during 7β-hydroxycholesterol and 7-ketocholesterol-induced apoptosis is caspase independent and is not required to trigger cell death. Cell Death Differ 2001;8:83–99.

[18] Kahn E, Lizard G, Frouin F, Bernengo JC, Souchier C, Bessède G, Clément O, Siitari H, Gambert P, Frija O, Todd-Pokropek A. Confocal analysis of phosphatidylserine externalization with the use of biotinylated Annexin V revealed with streptavidin-FITC, -europium, -phycoerythrin or Texas red in oxysterol-treated apoptotic cells. Anal Quant Cytol Histol 2001;23:47–55.

[19] Lizard G, Gueldry S, Sordet O, Monier S, Athias A, Miguet C, Bessède O, Lemaire S, Solary F, Gambert P. Glutathione is umplied in the control of 7-ketocholesterol-induced apoptosis, which is associated with radical oxygen species production. FABEB J 1998;12:1651–63.

[20] Lizard G, Miguet C, Bessède O, Monier S, Gueldry S, Néel D, Gambert P. Impairment with various antioxidants of the loss of mitochondrial transmembrane potential and of cytosolic release of cytochrome *c* occuring during 7-ketocholesterol-induced apoptosis. Free Radic Biol Med 2000;28:743–53.

[21] Minta JO, Pambrun L. *In vitro* induction of cytologic and functional differentiation of the immature human monocyte-like cell line U-937 with phorbol myristate acetate. Am J Pathol 1985;119:111–26.

[22] Donson AM, Baneijee A, Gamboni-Robertson F, Fleitz JM, Foreman NK. Protein kinase C isoform is critical for proliferation in human glioblastoma cell lines. J Neuro-Oncol 2000;47:109–15.

[23] Leveque D, Wihlm J, Jehl F. Pharmacology of Catharantus alkaloids. Bull Cancer 1996;83:176–86.

[24] Wills PW, Hickley R, Malkas L. Ara-C differentially affects multiprotein forms of human cell DNA polymerase. Cancer Chemother Pharmacol 2000;46:193–203.

[25] Vasquez D. Inhibitors of protein synthesis. FEBS Lett 1974;40:S63–84.

[26] Negri C, Bernardi R, Donzelli M, Scovassi AI. Induction of apoptotic cell death by topoisomerase IT inhibitors. Biochemistry 1995;77:893–9.

[27] Krajewska M, Wang HG, Krajewski S, Zapata J, Shabaik A, Gascoyne R, Reed JC. Immunohistochemical analysis of *in vivo* patterns of CPP32 (caspase-3), a cell death protease. Cancer Res 1997;57:1606–13.

[28] Kanai M, Uchida M, Hanai S, Uematsu N, Uchida K, Miwa M. Poly(ADP-ribose)polymerase localizes to the centrosomes and chromosomes. Biochem Biophys Res Commun 2000;278:385–9.

[29] Rothe G, Valet G. Flow cytometric analysis of respiratory burst activity in phagocytes with hydroethidine and 2′,7′-dichlorofluorecin. J Leukocyte Biol 1990;47:440–8.

[30] Ohkawa H, Ohishi N, Yagi K. Assay for lipid peroxides in animal tissues by thiobarbituric acid reaction. Anal Biochem 1979;95:351–8.

[31] Hariri M, Millane G, Guimond MP, Guay G, Dennis IW, Nabi IR. Biogenesis of multilamellar bodies *via* autophagy. Mol Biol Cell 2000;11:255–68.

[32] Lizard G, Moisant M, Cordelet C, Monier S, Gambert P, Lagrost L. Induction of similar features of apoptosis in human and bovine vascular endothelial cells treated by 7-ketocholesterol. J Pathol 1997;183:330–8.

[33] Biederbick A, Kern HF, Elsässer HP. Monodansylcadaverine (MDC) is a specific *in vivo* marker for autophagic vacuoles. Eur J Cell Biol 1995;66:3–14.

[34] Niemann A, Baltes J, Elsässer HP. Fluorescence properties and staining behavior of monodansylpentane, a structural homologue of the lysosomotropic agent monodansylcadaverine. J Histochem Cytochem 2001;49:177–85.

[35] Iuliano L, Michelella F, Maranghi M, Frati G, Diczfalusy U, Violi F. Bioavailability of Vitamin E as function of food intake in healthy subjects: effects on plasma peroxide-scavenging activity and cholesterol-oxidation products. Arterioscler Thromb Vasc Biol 2001;21:E34–7.

[36] Bron D, Asmis R. Vitamin E and the prevention of atherosclerosis. Int J Vitam Nutr Res 2001;71:18–24.

[37] Smith PK, Krohn RI, Hermanson GT, Mallia AK, Gartner FH, Provenzano MD, Fujimoto EK, Goeke NM, Olson BJ, KIenk DC. Measurement of protein using bicinchoninic acid. Anal Biochem 1985;150:76–85.

[38] Miller SA, Dykes DD, Polesky HF. A simple salting out procedure for extracting DNA for human nucleated cells. Nucl Acids Res 1988;16:1215.

[39] Chen LB. Mitochondrial membrane potential in living cells. Ann Rev Cell Biol 1988;4:155–81.

[40] Macho A, Hirsch T, Marzo I, Marchetti P, Dallaporta B, Susin SA, Zamzami N, Kroemer K. Glutathione depletion is an early and calcium elevation is a late event of thymocyte apoptosis. J Immunol 1997;158:4612–9.

[41] Bird RP, Draper HH. Comparative studies on different methods of malonaldehyde determination. Meth Enzymol 1984;105:299–305.

[42] Slee EA, Adrain C, Martin SJ. Serial killers: ordering caspase activation events in apoptosis. Cell Death Differ 1999;6:1067–74.

[43] Sun XM, MacFarlane M, Zhuang J, Wolf ZB, Green DR, Cohen GM. Distinct caspase cascades are initiated in receptor-mediated and chemical-induced apoptosis. J Biol Chem 1999;274:5053–60.
[44] Chandra J, Samali A, Orrenius S. Triggering and modulation of apoptosis by oxidative stress. Free Radic Biol Med 2000;29:323–33.
[45] Kannan K, Jain SK. Oxidative stress and apoptosis. Pathophysiology 2000;27:153–63.
[46] Mügge A. The role of reactive oxygen species in atherosclerosis. Z Kardiol 1998;87:851–64.
[47] Kockx MM. Apoptosis in the atherosclerotic plaque. Quantitative and qualitative aspects. Arterioscler Thromb Vasc Biol 1998;18:1519–22.
[48] Harangi M, Remenyik E, Seres I, Varga Z, Katona F, Paragh G. Determination of DNA damage induced by oxidative stress in hyperlipidemic patients. Mutat Res 2002;513:17–25.
[49] Colles SM, Irwin KC, Chisolm GM. Role of multiple oxidized LDL lipids in cellular injury: dominance of 7β-hydroperoxycholesterol. J Lipid Res 1996;37:2018–28.
[50] Bansal O, Singh U, Bansal MP. Effect of 7β-hydroxycholesterol on cellular redox status and heat shock protein 70 expression in macrophages. Cell Physiol Biochem 2001;11:241–6.
[51] O'Callaghan YC, Woods JA, O'Brien NM. Comparative study of the cytotoxicity and apoptosis-inducing potential of commonly occuring oxysterols. Cell Biol Toxicol 2001;17:127–37.
[52] Kroemer O, Petit P, Zamzami N, Vayssiere JL, Mignotte B. The biochemistry of programmed cell death. FASEB J 1995;9:1277–87.
[53] Cai J, Jones D. Superoxide in apoptosis. Mitochondrial generation triggered by cytochrome *c* loss. J Biol Chem 1998;273:11401–4.
[54] Kamata H, Hirata H. Redox regulation and cellular signalling. Cell Signal 1999;11:1–14.
[55] Meyer JW, Schmitt ME. A centarl role for the endothelial NADPH-oxidase in atherosclerosis. FEBS Lett 2000;472:1–4.
[56] Rosenblat M, Aviram M. Oxysterol-induced activation of macrophage NADPH-oxidase enhances cell-mediated oxidation of LDL in the atherosclerotic apoplipoprotein F deficient mouse: inhibitory role for Vitamin E. Atherosclerosis 2002;160:69–80.
[57] Hsieh CC, Yen MH, Yen CH, Lau YT. Oxidized low density lipoprotein induces apoptosis *via* generation of reactive oxygen species in vascular smooth muscle cells. Cardiovasc Res 2001;49:135–45.
[58] Hansson GK. Immune mechanisms in atherosclerosis. Arterioscler Thromb Vasc Biol 2000;21:1876–90.
[59] Fiers W, Beyaert R, Declercq W, Vandenabeele P. More than one way to die: apoptosis, necrosis and reactive oxygen damage. Oncogene 1999;18:7719–30.
[60] Stromhaug PE, Klionsky DI. Approaching the molecular mechanism of autophagy. Traffic 2001;2:524–31.
[61] Bursch W. The autophagosomal–lysosomal compartment in programmed cell death. Cell Death Differ 2001;8:569–81.
[62] Bustamante J, Tovar BA, Montero G, Boveris A. Early redox changes during rat thymocyte apoptosis. Arch Biochem Biophys 1997;337:121–8.
[63] Hall AG. The role of glutathione in the regulation of apoptosis. Eur J Clin Invest 1999;29:238–45.
[64] Sawada M, Nakashima S, Banno Y, Yamakawa H, Hayashi K, Takenaka K, Nishimura Y, Sakai N, Nozawa Y. Ordering of ceramide formation, caspase activation, Bax/Bcl-2 expression during etoposide-induced apoptosis in C6 glioma cells. Cell Death Differ 2000;7:761–72.
[65] Lizard G, Monier S, Cordelet C, Gesquière L, Deckert V, Gueldry S, Lagrost L, Gambert P. Characterization and comparison f the mode of cell death, apoptosis versus necrosis, induced by 7β-hydroxycholestrol and 7-ketocholestrol in the cells of the vascular wall. Arterioscler Thromb Vasc Biol 1999;10:1190–2000.
[66] Yin J, Chaufour X, McLachlan C, McGuire M, White G, King N, Hambly B. Apoptosis of vascular smooth muscle cells induced by cholesterol and its oxides *in vitro* and *in vivo*. Atherosclerosis 2000;148:365–74.